Dynamic Modeling and Control of the Planar Snake Robot Interacting with Obstacles in Dense Environments

Tianyu Wang

***Abstract*— In this work, we focus on developing a reliable dynamic model of multi-link snake robot locomotion and interaction with obstacles in dense environments, and designing controllers to achieve basic trajectory following objectives in simulations. Equations of motion, frictions, and contacts are modeled link-wise, and then combined to full dynamics of the whole articulated system. Partial feedback linearization method is used in the controller design to achieve varying gaits for reasonable movements of the snake robot. Reliability of the model and effectiveness of the controller are validated in demos, which enable a broader area for control strategy development in snake robots.**

I. INTRODUCTION

Snake robots are biomimetic robots can transverse complex terrains where traditional robots can hardly move. Plenty of previous works have shown different methods to achieve effective or efficient global objectives by leveraging the relative motion among the internal degree of freedoms during locomotion (Figure 1). One main approach to snake robot locomotion problem is based on the kinematic model of body shapes [1] [2] [3] [4]. But kinematic models will not work for the complex environment and not allow the snake robot to react to obstacles since it cannot tell how obstacles perturb the system. Dynamic models are developed to solve the locomotion problem in [5] [6] [7], introducing force control strategies into the snake robot control. [8] [9] consider the control problem when the snake robot is statically contacting with obstacles. However, how the irregular environment will affect the snake robot during locomotion and how snake robots can react to the obstacles to maintain its stable locomotion received limited focus in previous literature. In this work, we wish to first develop a reliable dynamic model of multi-link snake robot locomotion and interaction with obstacles, and then develop different control strategies that help the snake robot achieve better and more efficient locomotion in dense environments.

The report is organized as follows: Section II summarizes dynamic model derivation, including equations of motion of snake robot, modeling of frictions and modeling of collisions and contacts. Then, Section III develops basic controllers based on partial feedback linearization method to achieve reasonable locomotion. Section IV shows part of results of this work, validating the reliability of the model and effectiveness of the controller. Section V briefly discusses advantages and current drawbacks of this work, and concludes how we would like to move forward to the future work.

Tianyu Wang is with the Department of Mechanical Engineering, Carnegie Mellon University, tianyuw2@andrew.cmu.edu

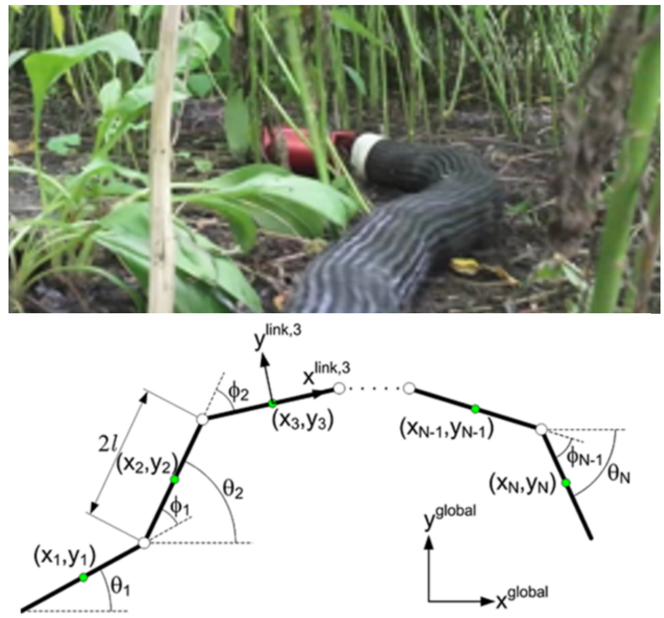

Fig. 1. Top: A photo of real snake robot locomotion in a dense environment; Bottom: A generalized multi-link model for planar snake robots [6].

II. DYNAMIC MODELING OF SNAKE MOTION

A planar snake robot with N links has $N-1$ actuated joints and $N+2$ degrees of freedom (Figure 1). Dynamics of this typical underactuated system can be very tedious, especially when it interacts with complex environments. To simplify the problem, we will construct the dynamic model of planar snake robots under assumptions as below.

- The snake is consist of $N \geq 3$ ideal and identical links. The centers of mass are located in the geometrical centers of the links. Each link has mass m, length $2l$, and moment of inertia I.
- Relative joint angles will stay in the range $[-90°, 90°]$.
- All the obstacles are convex and immovable. Contact is at a single point.
- Links and obstacles are perfect rigid bodies. They will not deform when collision happens.
- All the positions and geometric features of obstacles are known.
- Ground and obstacle friction can be modeled as viscous friction.

A. Equations of motion of the system

To derive the full dynamics of the planar snake robot with N links, based on simple dynamic model developed in [5], we started with equations of motion of link i. As shown in Figure 2, u_i and u_{i-1} are two input torques from rotary actuators at two ends of link i, forces g_{i-1} and g_i represent the inner-structure interaction forces between link $i-1$ and link i, link i and link $i+1$, force f_i and torque $\tau_{f,i}$ are the friction force and torque exerted by the ground, force $h_{i,k}$ and torque $\tau_{h,i,k}$ represent the contact force and torque exerted by obstacle k. Notice $h_{i,k}$ is consist of a normal contact force which prevents penetration and a tangential friction force which is proportional to the tangential velocity of link i. $h_{j,k}$ and $\tau_{h,j,k}$ are zeros when link j is not in contact with obstacle k. θ_i is the absolute angle of link i in the spatial frame and (x_i, y_i) is the position of center of mass in the spatial frame. From the free body diagram, we

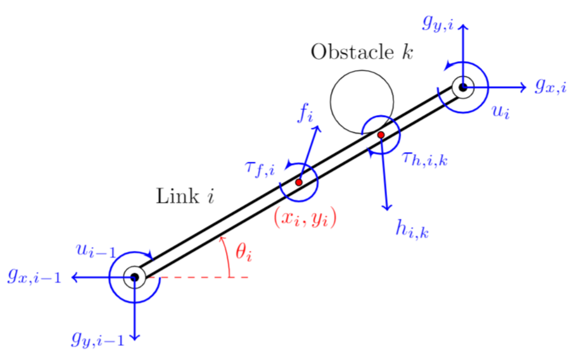

Fig. 2. Free body diagram of a single link.

can derive equation of motions of a single link as,

$$m\ddot{x}_i = f_{x,i} + h_{x,i,k} + g_{x,i} - g_{x,i-1}, \tag{1}$$
$$m\ddot{y}_i = f_{y,i} + h_{y,i,k} + g_{y,i} - g_{y,i-1}, \tag{2}$$
$$\begin{aligned} I\ddot{\theta}_i =& \tau_i - \tau_{i-1} + \tau_{f,i} + \tau_{h,i,k} \\ &- l\sin\theta_i(g_{x,i} + g_{x,i-1}) + l\cos\theta_i(g_{y,i} + g_{y,i-1}). \end{aligned} \tag{3}$$

From the multi-link structure, we will naturally have geometric constraints,

$$x_{i+1} - x_i = l(\cos(\theta_i) + \cos(\theta_{i+1})), \tag{4}$$
$$y_{i+1} - y_i = l(\sin(\theta_i) + \sin(\theta_{i+1})), \tag{5}$$

for all $i \in \{1, ..., N-1\}$. By collecting equations (1-3) and constraints (4, 5) for all links, we could cancel out all inner-structure interaction forces g_x and g_y using the geometric constraints. The full dynamics of the planar snake robot is in the form,

$$M(q)\ddot{q} + C(q,\dot{q}) + G(q)(f+h) + H(q)(\tau_f + \tau_h) = Bu, \tag{6}$$

where $q = [\phi_1, ..., \phi_{N-1}, \theta_N, x, y]^T$. ϕ_i is the joint angle between link i and link $i+1$, θ_N is the absolute angle of link N (so-called *heading angle*), x and y is the position of the center of mass of the snake robot in the spatial frame.

B. Modeling of ground friction

In this work, we used viscous friction model for ground frictions. The tangential and normal friction forces that ground exerting on the link are proportional to the velocity of the link in corresponding directions, with coefficients c_t and c_n. Integrating over the link, the total friction force and torque is given by,

$$f_i = -\mathbf{R}^{\text{spatial}}_{\text{link } i} \begin{bmatrix} c_t & 0 \\ 0 & c_n \end{bmatrix} \left(\mathbf{R}^{\text{spatial}}_{\text{link } i}\right)^T \begin{bmatrix} \dot{x}_i \\ \dot{y}_i \end{bmatrix}, \tag{7}$$
$$\tau_{f,i} = -c_n I\dot{\theta}_i, \tag{8}$$

where $\mathbf{R}^{\text{spatial}}_{\text{link } i}$ is the rotation matrix from link i local frame to spatial frame. Collect all friction forces and torques into vector form, and notice that f is related to state q and $\dot{q}$, τ_f is related only to $\dot{q}$. They can be written as functions of state,

$$f = F(q, \dot{q}), \tag{9}$$
$$\tau_f = T_f(\dot{q}). \tag{10}$$

C. Modeling of collision and contact

As all methods for modeling of collision and contact used in snake robot literature are not complete. We derived a full collision and contact model for unlimited collision and contact by inheriting ideas from [10]. When link i collides with obstacle k, link i will experience an instantaneous change in the velocity if there is a trend of penetration. Post-collision velocity v_i^+ and unit normal of collision surface $\hat{n}_k$ (pointing outward of the obstacle k) should fulfill the non-penetration constraint,

$$v_i^+ \cdot \hat{n}_k \geq 0. \tag{11}$$

This instantaneous velocity change is caused by an impulse $J_k = j_k\hat{n}_k$ exerted by obstacle k, in the direction of $\hat{n}_k$ with magnitude j_k. Using the information of pre-collision velocity of link i, magnitude j_k can be calculated as,

$$j_k = \frac{-(1+\epsilon)v_i^- \cdot \hat{n}_k}{\frac{1}{m} + \hat{n}_k \cdot (I^{-1}(r_i \times \hat{n}_k)) \times r_i}. \tag{12}$$

Details of the derivation of this formula is omitted because of space limitations. Here ϵ is the restitution coefficient which determines how much kinetic energy is lost, r_i is the vector from center of mass of link i to the collision position. Notice that, if $r_i \neq 0$, i.e., collision is not at the center of mass of link i, J_k produces an impulsive torque of

$$\tau_{J_k} = r_i \times J_k. \tag{13}$$

Then we can write the instantaneous changes in velocities of link i as,

$$v_i^+ = v_i^- + \frac{J_k}{m}, \tag{14}$$
$$\omega_i^+ = \omega_i^- + \frac{\tau_{J_k}}{I}. \tag{15}$$

By collecting the velocity changes over all the links and obstacles, we are able to write the state change in $\dot{q}$ as a mapping from pre-collision state to post-collision state,

$$\dot{q}^{+} = P(\dot{q}^{-}). \tag{16}$$

When link i is in contact with obstacle k, there exist an external contact force and torque acting by the obstacle, which makes sure there is no penetration. According to the properties of the contact, contact force and acceleration of the link should satisfy several constraints:

1) No net acceleration in the penetration direction $-\hat{n}_k$,

$$\dot{v_i} \cdot \hat{n}_k \geq 0. \tag{17}$$

2) Contact forces must always be repulsive, each contact force must act outward of the obstacle, in the form $h_{n,i,k}\hat{n}_k$ (subscript n means normal direction),

$$h_{n,i,k} \geq 0. \tag{18}$$

3) Contact force $h_{n,i,k}\hat{n}_k$ must become zero if contact is breaking,

$$h_{n,i,k}(\dot{v_i} \cdot \hat{n}_k) = 0. \tag{19}$$

Considering all contact forces exerted directly on link i, acceleration of link i can be written as

$$\dot{v_i} = a_{i1}h_{n,i,1} + a_{i2}h_{n,i,2} + \cdots + a_{im}h_{n,i,m} + b_i, \tag{20}$$

where b_i is contributions to acceleration by other forces. Collecting all equations over N links, we have

$$\dot{v} = \begin{bmatrix} \dot{v_1} \\ \vdots \\ \dot{v_N} \end{bmatrix} = A \begin{bmatrix} h_{n,1,1} & \cdots & h_{n,N,1} \\ \vdots & \ddots & \vdots \\ h_{n,1,m} & \cdots & h_{n,N,m} \end{bmatrix} + b. \tag{21}$$

Using constraint as stated in (17), we are able to solve all unknown magnitudes of contact forces $h_{n,i,k}$.

Friction between obstacles and links is also considered to be viscous type. Similar to ground friction,

$$h_{t,i,k} = -\mathbf{R}^{\text{spatial}}_{\text{obstacle } k} \begin{bmatrix} \mu_t & 0 \\ 0 & 0 \end{bmatrix} \left(\mathbf{R}^{\text{spatial}}_{\text{obstacle } k}\right)^T \begin{bmatrix} \dot{x}_i \\ \dot{y}_i \end{bmatrix}, \tag{22}$$

where subscript t in $h_{t,i,k}$ means tangential direction, $\mathbf{R}^{\text{spatial}}_{\text{obstacle } k}$ is the rotation matrix from obstacle k local frame to spatial frame. Thus, the final form of the contact forces will be functions of state q and $\dot{q}$ as well,

$$h = H_n(q, \dot{q}) + H_t(\dot{q}) = H(q, \dot{q}), \tag{23}$$

$$\tau_h = T_h(q, \dot{q}). \tag{24}$$

Substituting (9, 10, 23, 24) into (6), we will have the final form of the dynamics,

$$\tilde{M}(q)\ddot{q} + \tilde{C}(q, \dot{q}) + \tilde{K}(q) = \tilde{B}u. \tag{25}$$

This equation of motion can be used in both contact mode and non-contact mode. Notice that in non-contact mode, contact forces are simply zeros.

III. CONTROLLER DESIGN

A. Partial feedback linearization

If our purpose is to control the snake robot to move from one location to another location, we need to consider how we can leverage $N-1$ control inputs to move the position of its center of mass to a desired point. Since this is an underactuated system, position of center of mass is not directed actuated, the strategy we used here is partial feedback linearization. The state q is divided into actuated state $q_a = [\phi_1, ..., \phi_{N-1}]^T$ and unactuated state $q_u = [\theta_N, x, y]^T$. Then dynamics in (25) can be divided as

$$M_{11}\ddot{q_a} + M_{12}\ddot{q_u} + C_1 + K_1 = u, \tag{26}$$

$$M_{21}\ddot{q_a} + M_{22}\ddot{q_u} + C_2 + K_2 = 0. \tag{27}$$

Using (27) to cancel out $\ddot{q_u}$ in (26), we have

$$\begin{aligned}(M_{11} - M_{12}M_{22}^{-1}M_{21})\ddot{q_a} + C_1 + K_1 \\ -M_{12}M_{22}^{-1}(C_2 + K_2) = u.\end{aligned} \tag{28}$$

If we let

$$\begin{aligned}u = (M_{11} - M_{12}M_{22}^{-1}M_{21})\bar{u} + C_1 + K_1 \\ -M_{12}M_{22}^{-1}(C_2 + K_2),\end{aligned} \tag{29}$$

dynamics is in the form

$$\begin{cases} \ddot{q_a} = \bar{u} \\ \ddot{q_u} = \mathcal{A}(q, \dot{q}) + \mathcal{B}(q_a)\bar{u} \end{cases} \tag{30}$$

We thus can freely design $\bar{u}$ to generalize different gaits for locomotion because $\bar{u}$ directly controls the joint angles.

B. Lateral undulation

As discussed in [1],[2], snakes will generate an overall forward movement when it employs a lateral undulation gait. To mimic lateral undulation in the snake body, we let the snake robot produce continuous waves that are propagated along its body, by moving the joint angles according to the reference

$$\phi_{i,\text{ref}} = \alpha \sin(\omega t + (i-1)\delta) + \beta, \tag{31}$$

where β is a constant offset controlling the direction of snake movement, α is amplitude, ω is temporal frequency, and t is time. The spatial frequency δ determines the number of waves on the snake robots body. The parameters in the reference can be changed to create varying behaviors. In the implementation of trajectory following that is introduced in the following section, we mainly tuned parameter β to keep the snake robot always heading to the target position.

C. PD controller

As discussed in part A, we are able to design $\bar{u}$ to implement lateral undulation on the snake robot. A PD-type controller was designed as

$$\bar{u} = k_p(\phi_{\text{ref}} - q_a) - k_d\dot{q_a}. \tag{32}$$

Using (29), we can eventually calculate the input u that controls the snake to generate lateral undulation behavior.

IV. RESULTS

A. Validation of the dynamic model

Video 1 in the appendix shows how the snake robot is going through a dense pegboard and getting to the target position. This video validates our modeling of snake robot and its interaction with obstacles in the environment. Also, as shown in Figure 3, the trajectory of snake center of mass without obstacles is smooth, while the trajectory becomes sharp when perturbed by collisions and contacts with the existence of obstacles.

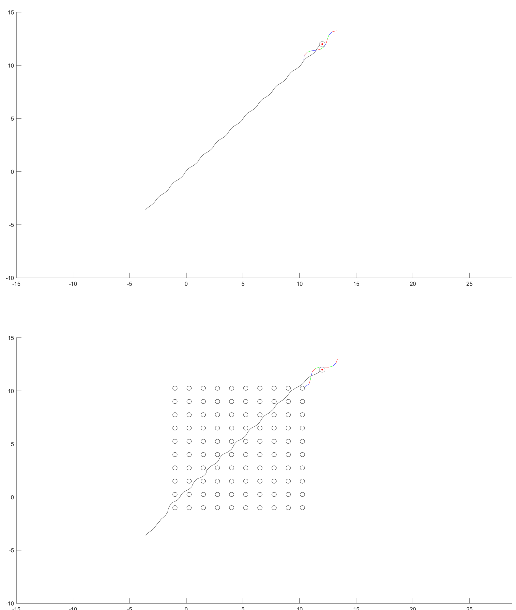

Fig. 3. Top: Trajectory of snake center of mass without obstacles; Bottom: Trajectory of snake center of mass with obstacles.

B. Trajectory following

Based on the low-level PD controller as stated in the previous section, a higher-level planner is designed for global motion planning. Using this higher-level planner, the snake robot is able to follow a sequence of pre-selected targets positions or a pre-defined trajectory for the center of mass. The main approach of this high-level planner is to design state feedback for the parameter β in the joint angle references. Video 2 in the appendix shows the process of selecting the sequence of target positions, trajectory converging to each target, and eventually reaching the final target. Figure 4 shows the output trajectory of snake center of mass.

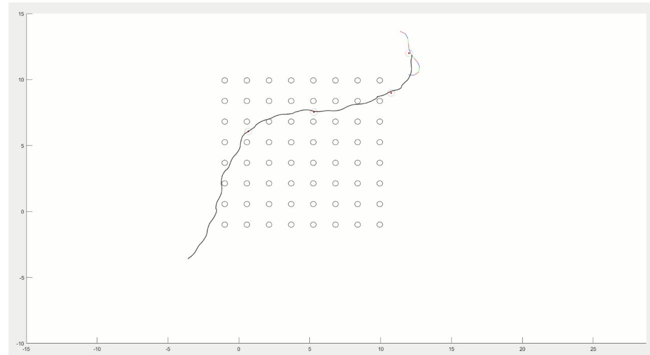

Fig. 4. Discrete trajectory following.

V. DISCUSSION

Compared to existing snake robot simulators based on kinematic models [1][2][3], this work develops a full dynamic model for the snake robots and also enables collisions and contacts with obstacles. The dynamic model will make the force control on snake robots possible. Compared to the simple contact force model discussed in [6][8], this work enables the snake robot to have multiple contacts at the same time, which is usually the case when locomoting in a dense environment. The PD-type controller allows the reference of joint angles to be discontinuous, which is very easy to implement. However, this controller makes the snake robot unable to track time-varying references perfectly, which is also the reason why we did not show a continuous trajectory following case in the results.

Future work will focus on developing better low-level controllers for continuous trajectory tracking. We will study how obstacles perturb the system during the trajectory tracking and come up with control strategies to make locomotion more efficient. Moreover, with the dynamic model, we are able to formulate optimal control problem to optimize the control usage during locomotion.

APPENDIX

1) Video 1: https://drive.google.com/file/d/1b3eRfCfWzLuVMfayiwNoW9qh4yt9Iq_P/view?usp=sharing
2) Video 2: https://drive.google.com/file/d/1ko_XHhVUFRnnhtN6MqohhfMgKhe9Rl7A/view?usp=sharing

ACKNOWLEDGMENT

The author is grateful for discussion and help from Professor Howie Choset, Matthew Travers, and other colleagues in the lab.

REFERENCES

[1] Hirose S. Biologically inspired robots: snake-like locomotors and manipulators. Oxford: Oxford university press; 1993.

[2] Whitman J, Ruscelli F, Travers M, Choset H. Shape-based compliant control with variable coordination centralization on a snake robot. In2016 IEEE 55th Conference on Decision and Control (CDC) 2016 Dec 12 (pp. 5165-5170). IEEE.

[3] Dear T, Kelly SD, Travers M, Choset H. Locomotion of a Multi-Link Nonholonomic Snake Robot. InASME 2017 Dynamic Systems and Control Conference 2017 Oct 11 (pp. V002T21A011-V002T21A011). American Society of Mechanical Engineers.

[4] Hatton RL, Choset H. Geometric motion planning: The local connection, Stokes theorem, and the importance of coordinate choice. The International Journal of Robotics Research. 2011 Jul;30(8):988-1014.

[5] Saito M, Fukaya M, Iwasaki T. Modeling, analysis, and synthesis of serpentine locomotion with a multilink robotic snake. IEEE control systems magazine. 2002 Jan;22(1):64-81.

[6] Liljeback P, Pettersen KY, Stavdahl O, Gravdahl JT. Snake robots: modelling, mechatronics, and control. Springer Science & Business Media; 2012 Jun 13.

[7] Rollinson D, Alwala KV, Zevallos N, Choset H. Torque control strategies for snake robots. In2014 IEEE/RSJ International Conference on Intelligent Robots and Systems 2014 Sep 14 (pp. 1093-1099). IEEE.

[8] Liljeback P, Pettersen KY, Stavdahl O. Modelling and control of obstacle-aided snake robot locomotion based on jam resolution. In2009 IEEE International Conference on Robotics and Automation 2009 May 12 (pp. 3807-3814). IEEE.

[9] Holden C, Stavdahl , Gravdahl JT. Optimal dynamic force mapping for obstacle-aided locomotion in 2d snake robots. In2014 IEEE/RSJ International Conference on Intelligent Robots and Systems 2014 Sep 14 (pp. 321-328). IEEE.

[10] Baraff D. An introduction to physically based modeling: rigid body simulation IInonpenetration constraints. SIGGRAPH course notes. 1997:D31-68.